PAPER

Check for updates

Akkermansia muciniphila attenuated lipopolysaccharide-induced acute lung injury by modulating the gut microbiota and SCFAs in mice†

Jian Shen,‡[a] Shuting Wang,‡[b] He Xia,[a] Shengyi Han, [ID][a] Qiangqiang Wang,[a] Zhengjie Wu,[a] Aoxiang Zhuge,[a] Shengjie Li,[a] Hui Chen,[a] Longxian Lv, [ID][a] Yanfei Chen[a] and Lanjuan Li [ID] *[a,c]

Gut microbiota are closely related to lipopolysaccharide (LPS)-induced acute lung injury (ALI). *Akkermansia muciniphila* (*A. muciniphila*) maintains the intestinal barrier function and regulates the balance of reduced glutathione/oxidized glutathione. However, it may be useful as a treatment strategy for LPS-induced lung injury. Our study aimed to explore whether *A. muciniphila* could improve lung injury by affecting the gut microbiota. The administration of *A. muciniphila* effectively attenuated lung injury tissue damage and significantly decreased the oxidative stress and inflammatory reaction induced by LPS, with lower levels of myeloperoxidase (MDA), enhanced superoxide dismutase (SOD) activity, decreased pro-inflammatory cytokine levels, and reduced macrophage and neutrophil infiltration. Moreover, *A. muciniphila* maintained the intestinal barrier function, reshaped the disordered microbial community, and promoted the secretion of short-chain fatty acids (SCFAs). *A. muciniphila* significantly downregulated the expression of TLR2, MyD88 and NF-kappa B ($P < 0.05$). Butyrate supplementation demonstrated a significant improvement in the inflammatory response ($P < 0.05$) and mitigation of histopathological damage in mice with ALI, thereby restoring the intestinal butyric acid concentration. In conclusion, our findings indicate that *A. muciniphila* inhibits the accumulation of inflammatory cytokines and attenuates the activation of the TLR2/Myd88/NF-κB pathway due to exerting anti-inflammatory effects through butyrate. This study provides an experimental foundation for the potential application of *A. muciniphila* and butyrate in the prevention and treatment of ALI.

Introduction

Acute lung injury (ALI) is defined as acute, diffuse, and inflammatory lung injury characterized by a variety of pathogenic factors, such as mechanical trauma, bacteria, and viruses (such as SARS CoV-2), which can cause noncardiac edema, hypoxemia, and the inflammatory infiltration of lung diseases.[1,2] ALI is prone to developing into acute respiratory distress syndrome (ARDS).[3] As previously reported, the inci-

[a]*State Key Laboratory for Diagnosis and Treatment of Infectious Diseases, National Clinical Research Centre for Infectious Diseases, Collaborative Innovation Centre for Diagnosis and Treatment of Infectious Diseases, The First Affiliated Hospital, Zhejiang University School of Medicine, 79 Qingchun Rd., Hangzhou City 310003, China. E-mail: ljli@zju.edu.cn; Fax: +86-571-87236459; Tel: +86-571-87236458*
[b]*Department of Gastroenterology, The Second Affiliated Hospital of Nanchang University, Jiangxi, Nanchang 330006, China*
[c]*Jinan Microecological Biomedicine Shandong Laboratory, Jinan, China*
†Electronic supplementary information (ESI) available. See DOI: https://doi.org/10.1039/d3fo04051h
‡These authors are contributed equally to this study.

dence rates of ALI and ARDS in patients over 15 years of age are 78.9 and 58.7 cases per 100 000 people per year, respectively, and the mortality rates are 38.5% and 41.1%, respectively, in the USA.[3] ALI and ARDS are characterized by severe acute inflammatory reactions, leading to increased permeability of pulmonary capillaries, and injury of alveolar epithelial cells and endothelial cells. Continuous and repeated injury can induce tissue and cellular responses, which ultimately lead to pulmonary fibrosis.[4] The current clinical treatment of ALI/ARDS is symptomatic treatment, such as mechanical ventilation and fluid management supplemented with glucocorticoids, inhaled pulmonary vasodilators and extracorporeal membrane oxygenation.[6] Currently, due to the lack of effective treatment strategies, the prognosis of ALI/ARDS for most patients is poor. Furthermore, studies have reported that intestinal microbiota imbalance is associated with an increased mortality rate caused by respiratory infections. In particular, the gut–lung axis may have a crucial effect on the pathological immune response to SARS-CoV-2.[7] Recently, domestic and foreign scholars have noted that probiotic sup-

plements can significantly improve symptoms, increase the virus clearance rate, and rebuild the intestinal microbiota in COVID-19 patients.[8–10] In summary, multiple research reports suggest that the gut microbiota plays a crucial role in the prevention and treatment of ALI.

Recently, the potential role of the gut microbiota and its metabolites in the progression of ALI has gradually been revealed. Our research team previously demonstrated extensive alterations in the gut microbiota of COVID-19 patients, which were closely related to their immune response and disease severity.[11–13] We proposed that the relative abundance of microbes producing short chain fatty acids (SCFAs), such as *Bifidobacterium*, *Akkermansia muciniphila*, *etc.*, which are negatively associated with changes in serum cytokines, was reduced in COVID-19 patients and even those with critical illness, and was associated with changes in serum cytokines.[13] Zhang *et al.* reported that the concentrations of SCFAs and ʟ-isoleucine in the feces of COVID-19 patients were still significantly decreased after the disease improved.[14] Moreover, Wang *et al.* revealed that succinic acid derived from the gut microbiota exacerbated ALI induced by intestinal ischemia/reperfusion by promoting polarization of alveolar macrophages.[15] Additionally, an observational study revealed that the pulmonary microbiome can be treated as a potential marker to predict the clinical outcome of critically ill patients, and provided a new preventive treatment target for ARDS.[16] In summary, the gut–lung axis may play a role in the pathogenesis of ALI, and previous studies have shown that antibiotic cocktail (ABX)-induced microbial depletion can alleviate symptoms of lipopolysaccharide (LPS)-induced ALI in mice through the gut–lung axis.[17] A four-blind clinical study indicated that probiotics (including 3 strains of *Lactobacillus plantarum* and 1 strain of *Lactococcus lactis*) were more effective in improving lung infiltration, and shortening the duration of digestive and nondigestive symptoms.[8] Probiotics (or products) can be used to regulate the lung and intestinal microbiota, providing a new perspective for the prevention and treatment of ALI. Unfortunately, only a few probiotics have been proven to have protective effects on ALI.

Akkermansia muciniphila (*A. muciniphila*) adheres to the mucus layer, participates in the production of SCFAs, and regulates gene expression related to lipid metabolism and immune response.[18] Our research team has already found that *A. muciniphila* plays a vital role in maintaining the balance of intestinal microbiota, and its intervention could significantly ameliorate resistance to *Clostridium difficile* infection,[19] liver injury induced by concanavalin A,[20] and acetaminophen-induced liver injury.[21] Interestingly, *A. muciniphila* intervention can reduce acetaminophen-induced oxidative stress and inflammatory reactions by regulating the balance of reduced glutathione/oxidized glutathione, enhancing the activity of superoxide dismutase, maintaining the intestinal barrier function, reshaping the disturbed microbial community, and promoting the secretion of SCFAs (mainly acetic acid, propionic acid and butyric acid). Herein, the purpose of this study was to investigate the effect of *A. muciniphila* on LPS-induced lung

injury, and to determine the mechanism through integrated multi-omics analyses, including 16S sequencing, transcriptomics and metabolomics.

Methods

Strain and culture conditions

The probiotic strain *Akkermansia muciniphila* Muc^T was purchased from ATCC (number: BAA-835), and cultured anaerobically in brain heart infusion (BHI) medium at 37 °C for 48 h. The culture medium was centrifuged at 8000g for 10 min at 4 °C, followed by washing the precipitate twice and resuspension in PBS at 3×10^9 colony-forming units (CFU) per mL for gavage.

Animal model and experimental design

The ALI model was induced by intratracheal administration of LPS (derived from *Escherichia coli* 0111: B4, Sigma-Aldrich, Poole, United Kingdom).[5] Twenty-four 6- to 8-week-old C57BL/6 male mice (Shanghai SLAC Laboratory Animal Co. Ltd, China) were housed in a specific pathogen-free (SPF) environment with a 12 h light/dark cycle and a constant temperature of 22 ± 2 °C. After one week of adaptive feeding, mice were randomly divided into three groups ($n = 8$ per group) (Fig. 1A): NC (PBS + saline) group, PC (PBS + LPS) group, and AKK (AKK + LPS) group. The AKK group mice were treated with 0.2 ml of freshly prepared *A. muciniphila* suspension daily, while the NC and PC groups were administered 0.2 ml of PBS daily as a placebo for 21 days. On day 22, mice in the LPS and AKK groups were induced with 5 mg kg⁻¹ LPS, and mice in the NC group received an equal volume of PBS. After 5 days, the mice were euthanized and bronchoalveolar lavage fluid (BALF) was collected by washing the left lung with PBS through a tracheal tube. In addition, blood, lung and intestinal tissue samples were collected for subsequent analysis.

Animal histopathological evaluation

After fixation of lung and intestinal tissue samples with neutral formalin fixative for 24 hours, the tissues were embedded in paraffin, cut into 2 μm sections and stained with hematoxylin and eosin (H&E). Lung tissue sections were stained with antibodies against F4/80, myeloperoxidase (MPO) and lymphocyte antigen 6G (LY6G). Colon tissue sections were stained with zonula occludens-1 (ZO-1) and occludin antibodies to assess the intestinal barrier. Five representative fields of view were randomly chosen at 40× magnification in each sample. Quantification of the above staining was performed by calculating the percentage of positive area in the field of view using ImageJ. Pathology scores were assessed in a double-blind manner by two independent pathology professors.

Calculation of the W/D ratio of lung tissue

The right middle lobe of the mouse lung was collected, removed and dried with absorbent paper for immediate measurement of wet weight (W), and then dried in an oven at
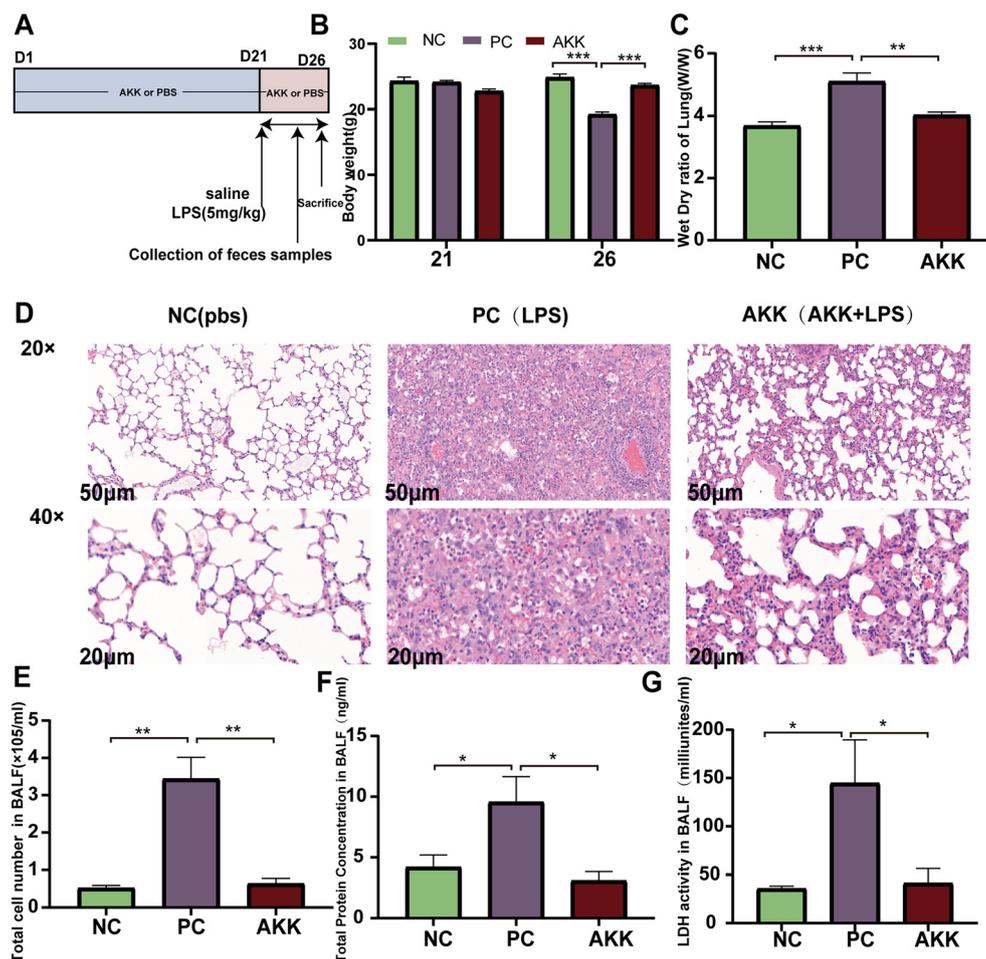
Fig. 1 *A. muciniphila* alleviated the lung injury induced by lipopolysaccharide. Experimental flowchart (A); changes in body weight (B) and lung dry wet ratio in mice (C) and (D), representative images of HE staining in lung tissue (scale = 50 μm); concentration of total protein (F), total cell count (E), and LDH activity (G) in bronchoalveolar lavage fluid (BALF); data are presented as the mean ± standard error of the mean (mean ± SEM); compared with the PC group, *$p < 0.05$, **$p < 0.01$, and ***$p < 0.001$. NC, PBS + saline group; PC, PBS + LPS group; AKK, *A. muciniphila* + LPS group. $n = 8$ each group.

70 °C for 72 hours for dry weight (D) measurement. Tissue edema was assessed by calculating the W/D ratio.

Lung tissue ELISA

MDA and SOD concentrations in lung tissue were measured by using a lipid peroxidation (MDA) assay kit and a superoxide dismutase (SOD) assay kit. Instructions in the kit manual were followed for operations.

BALF assay analysis

The collected BALF was centrifuged at 800g for 10 min below 4 °C and the supernatant was stored at −80 °C for subsequent analysis. Erythrocytes in the cell precipitate were lysed and later resuspended in 1000 μl PBS for cell counting using a countess automated cell counter (Thermo Fisher Scientific). The total protein content in BALF was determined using the Pierce™ BCA protein assay kit. In addition, the levels of lactate dehydrogenase (LDH), IL-1β and IL-6 in BALF were tested

using ELISA kits by following the instruction manual for the operation steps.

Analysis of serum parameters

The collected blood was centrifuged at 3000g for 15 min to obtain serum for subsequent analysis. The LPS binding protein (LBP) concentration was assessed using an enzyme-linked immunosorbent assay (ELISA) kit. Serum inflammatory cytokines were measured by the mouse cytokine 23-Plex assay kit. All operations were carried out according to the kit manual.

***A. muciniphila* quantification**

DNA was extracted from feces by the DNeasy PowerSoil Pro kit (Qiagen, Hilden, Germany). Primers (Table S1†) were used to detect and quantify *A. muciniphila* in feces. The standard curve was quantified using serial dilutions of isolated DNA.

Quantification of SCFAs in colonic contents

Colonic contents were mixed with 300 µl of 50% acetonitrile–water solution (v/v with internal standards [2H9]-pentanoic acid, [2H11]-hexanoic acid). After the samples were ground and extracted by sonication in an ice-water bath, samples were centrifuged at 12 000 rpm and 4 °C for 10 min, and the supernatant was diluted 5-fold with 50% acetonitrile–water solution (v/v). The samples were later derivatized and analyzed by UPLC-ESI-MS/MS for the qualitative and quantitative determination of the target metabolites.

RNA extraction and real-time fluorescence quantitative PCR analysis

RNA was extracted from lung and ileal tissue using the RNeasy plus mini kit (Qiagen, Valencia, CA, United States), according to the manufacturer's method. RNA was then converted to cDNA using the PrimeScript RT master kit (Takara Biomedicals, Kusatsu, Japan). Subsequently, mRNA was carried out using Premix Ex Taq (Takara Biomedicals, Kusatsu, Japan) in a ViiA7 real-time PCR system (Applied Biosystems, Waltham, Massachusetts, USA). The mRNA expression was measured, and the control for the target gene expression level was the expression of Gapdh and β-actin. The gene primer sequences used for RT-qPCR analysis are shown in Table S1.†

16S rRNA sequencing

We collected mouse lung tissue and feces from which DNA was extracted by the DNeasy PowerSoil Pro kit (Qiagen, Hilden, Germany). The DNA extracted from lung tissue was amplified using primers (Table S1†) for amplification of the full length of the gene, followed by PCR amplification using primers (Table S1†) for the variable region V3 to V4 of the 16S rRNA gene. The DNA derived from feces was amplified using universal primers, which is shown in Table S1.† After identification, the data were sequenced on the Illumina NovaSeq6000 platform (Illumina Inc., CA, USA) and libraries were constructed.

The data were imported into QIIME2 for processing. By using the DADA2 plugin, the data were then clustered into amplicon sequence variant (ASV) groups and classified according to the Silva 138 database in QIIME2. Finally, the alpha diversity and beta diversity were assessed through QIIME2 software. The differences between taxa were also analyzed using linear discriminant analysis (LDA) effect sizes (LEfSe).

Lung transcriptome analysis

Lung tissue RNA quantification, library creation and sequencing were performed, as previously described.[22] Differential transcript analysis between groups was later performed using the R package DESeq2, and the P values obtained were adjusted to control for error incidence by using Benjamini and Hochberg's approach. Genes with $P_{adj} < 0.05$ by DESeq2 were considered as having differential transcripts.

Statistical analysis

Data were analyzed by SPSS 22.0 software (SPSS Inc., Chicago, IL), and the results are expressed as the mean ± standard error of the mean (SEM). The normality of the data was first tested by the Shapiro–Wilk test, and then the Mann–Whitney U test (for nonnormal distributions) or Student's t test (for normal distributions) was used to assess differences between the groups. Results with $P < 0.05$ were considered statistically significant. Images were prepared in GraphPad Prism 9.0 and R (version 4.2).

Results

A. muciniphila effectively protected against LPS-induced lung injury

We established a stable ALI mouse model by intratracheal injection of 5 mg kg^{-1} LPS. As shown in Fig. 1B, preintervention with *A. muciniphila* did not affect the body weight (BW) of mice in 21 days ($P > 0.05$). Before sacrificing the mice, the BW of mice in the PC group was again significantly lower than that in the NC group ($P < 0.001$), while preintervention with *A. muciniphila* maintained the BW of mice (AKK *vs.* NC, $P > 0.05$). The pathological changes in the lungs were estimated by H&E staining (Fig. 1D). As shown in Fig. 1D, diffuse alveolar and interstitial infiltration and alveolar wall and interstitial thickening were observed in the PC group. Conversely, the alveolar walls and interstation were thinner and the immune cell infiltration was lower in the AKK group than in the PC group. Additionally, the degree of pulmonary edema was analyzed by measuring the W/D ratio of the lung tissue. As shown in Fig. 1C, the W/D ratio of the LPS-treated mice was higher ($P < 0.001$), while the W/D ratio of the AKK group was lower than that of the PC group ($P < 0.01$).

To assess the alveolar barrier integrity, BALF was collected to measure the total protein levels (Fig. 1F), cell count (Fig. 1E), and LDH activity (Fig. 1G). The cell count, total protein level, and LDH activity in the PC group were significantly increased (PC *vs.* NC, $P < 0.01$, $P < 0.05$, $P < 0.05$, respectively), and the indicators mentioned above were all substantially reduced in the AKK group (AKK *vs.* PC, $P < 0.01$, $P < 0.05$, $P < 0.05$, respectively). Generally, *A. muciniphila* alleviates inflammatory cell infiltration, pulmonary hydroncus, and the permeability of the alveolar epithelial barrier in LPS-induced mice.

A. muciniphila reduced LPS-induced inflammatory responses

The LPS-induced lung injury model was reported to be characterized by both direct damage to capillary endothelial cells and concomitant inflammatory response, the degree of which can be evaluated by measuring inflammatory markers in the alveolar lavage fluid and serum. First, cytokine chip technology was utilized to test the levels of peripheral inflammatory factors and chemokines in serum. As shown in Fig. 2C–F, the levels of pro-inflammatory factors, including IL-1β ($P < 0.001$), IL-6 ($P < 0.001$), MCP1 ($P < 0.5$) and MIP-1α ($P < 0.001$), were
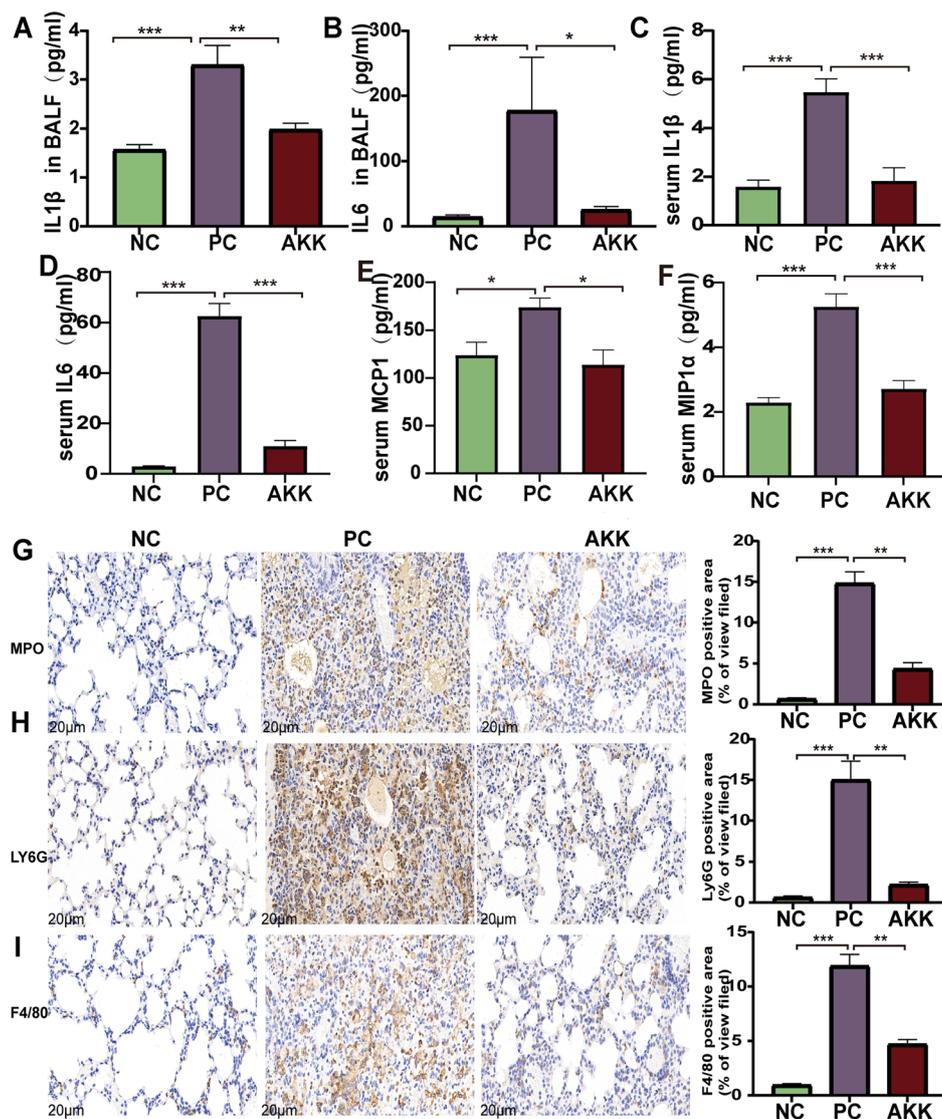
Fig. 2 *A. muciniphila* reduced inflammatory responses by lipopolysaccharide. IL-1β (A) and IL-6 (B) concentrations in bronchoalveolar lavage fluid (BALF); serum levels of IL-1β (C) IL-6 (D), MCP1 (E), and MIP-1α (F) (n = 8 each group). Representative images of MPO (G), Ly6G (H), and F4/80 (I) immunohistochemical staining (scale = 20 μm); n = 3 per group and five randomly selected visual fields. Data are shown as the mean ± standard error of the mean (mean ± SEM); compared with the PC group, *$p < 0.05$, **$p < 0.01$, and ***$p < 0.001$. NC, PBS + saline group; PC, PBS + LPS group; AKK, *A. muciniphila* + LPS group.

higher in the PC group than in the NC group. Additionally, they were remarkably decreased after intervention with *A. muciniphila* ($P < 0.05$). Notably, the IL-1β ($P < 0.001$) and IL-6 ($P < 0.001$) levels were also higher in the alveolar lavage fluid in the PC group than in the NC group (Fig. 2A and B), while the levels of the above factors were much lower in the AKK group than in the PC group ($P < 0.05$).

Furthermore, immunohistochemical analysis was performed using anti-F4/80, anti-MPO, and anti-Ly6G antibodies to estimate the lung infiltration by macrophages and neutrophils (Fig. 2G–J). The staining results showed that LPS significantly enhanced the recruitment of macrophages and neutrophils (NC *vs.* PC: $P < 0.001$, $P < 0.001$, $P < 0.001$, respectively), while *A. muciniphila* significantly improved the infiltration of

macrophages and neutrophils (AKK *vs.* PC: $P < 0.01$, $P < 0.01$, $P < 0.01$, respectively). These results indicate that *A. muciniphila* improved the pulmonary inflammatory response caused by LPS.

A. muciniphila improved the gut barrier function and inhibited lipopolysaccharide stimulation

The complex formed by the binding of LBP and LPS rapidly binds to CD14 detected on the surface of cells, which induces the production of cytokines.[23] The concentration of serum LBP was measured as a marker of systemic LPS exposure (Fig. 3E). Tissue oxidative damage plays a critical role in LPS-induced ALI mice. Compared to the NC group, the serum LBP levels in mice in the PC group was substantially increased ($P < 0.001$).
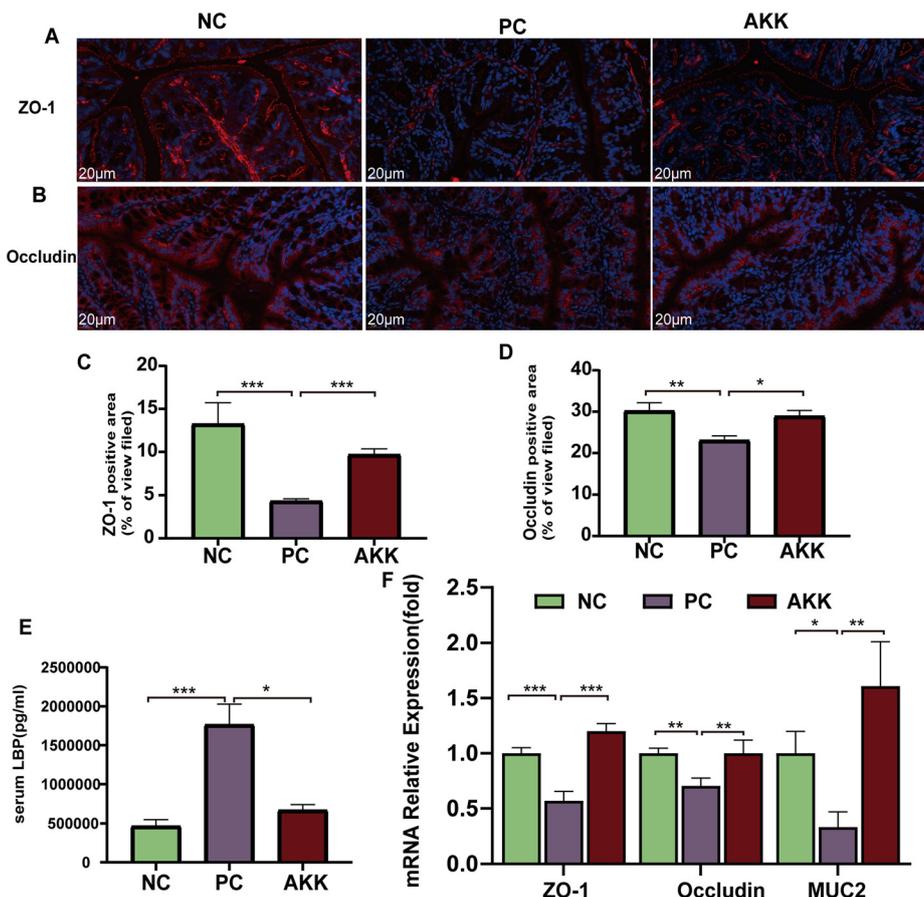
Fig. 3 *A. muciniphila* improved gut barrier function and inhibited lipopolysaccharide stimulation. Representative images of ZO-1 (A) and occludin (B) immunohistochemical staining (scale = 20 μm). By using ImageJ, the percentage of positive area (ZO-1 and occludin, respectively) was calculated; $n = 3$ per group and five randomly selected visual fields (C and D). Serum LBP (E) levels were measured by ELISA ($n = 8$ each group). (F) The mRNA expression levels of ZO-1, occluding, and MUC2 were normalized to Gapdh mRNA levels ($n = 8$ each group). Data are shown as the mean ± standard error of the mean (mean ± SEM); compared with the PC group, $*p < 0.05$, $**p < 0.01$, and $***p < 0.001$. NC, PBS + saline group; PC, PBS + LPS group; AKK, *A. muciniphila* + LPS group.

In contrast, the serum LBP concentration in the AKK group was lower ($P < 0.05$) than that in the PC group.

Systemic inflammation caused by lung injury resulted in the destruction of the integrity of the intestinal barrier, which allowed for the translocation of microbes and their products.[24] We used immunofluorescence to measure the protein expression levels of several typical intestinal barrier factors (ZO-1 and occludin) (Fig. 3A–D). The comparison between the NC and PC groups showed that LPS significantly reduced the levels of the ZO-1 ($P < 0.001$) and occludin ($P < 0.01$) proteins. Notably, *A. muciniphila* led to significantly higher levels of ZO-1 ($P < 0.001$) and occludin ($P < 0.05$) than in the PC group. Moreover, there was lower expression of ZO-1 ($P < 0.001$), occludin ($P < 0.01$), and MUC2 ($P < 0.05$) in the PC group than in the NC group, while AKK caused significantly higher expression levels of ZO-1 ($P < 0.001$), occludin ($P < 0.01$), and MUC2 ($P < 0.01$) at the mRNA level in colonic tissue than in the PC group (Fig. 3F). Briefly, *A. muciniphila* could ameliorate intestinal barrier dysfunction, which was closely related to the translocation of gut microflora.

A. muciniphila reshaped the gut microbiota of mice

To further explore the effect of *A. muciniphila* intervention on the gut flora of ALI mice, this study used 16S rRNA amplification sequence analysis on the colon fecal DNA of mice from each group. A total of 1 917 371 sequences of raw reads were captured from the sequencing of 24 samples. After quality filtering of the sequences, the total reads of nonchimeric reads in the NC, PC, and AKK groups were 431 808, 392 181, and 505 190, respectively. Our study revealed that under LPS stimulation, the alpha-diversity index (including Chao1 index, observed species indexes, Shannon index, and Simpson index) of the gut microbiota was significantly lower ($P < 0.05$), while the diversity index was higher ($P > 0.05$) in the AKK group than in the PC group (ESI Fig. 1†). PCoA based on unweighted UniFrac distances was carried out to evaluate the beta diversity of the gut microbiota. Community structure tests among different groups were performed with PERMANOVA analysis. As shown in the ESI Fig. 2A,† PC1 and PC2 explained 16.15% and 8.35% of the variation observed, respectively. The

microbial groups in the AKK, NC, and PC groups were significantly separated (PERMANOVA, $P = 0.001$).

Microbial community abundance and composition also shifted. The ESI Fig. 2B† shows that 8 bacterial phyla significantly differed among the groups. At the phylum level, compared with the NC group, the relative abundances of *Bacteroidotas* (57.09% *vs.* 66.29%, $P > 0.05$) and *Fusobacteriata* (0.02% *vs.* 0.05%, $P = 0.079$) showed an increasing trend, while the relative abundances of *Campilobacterium* (4.3% *vs.* 0.94%, $P = 0.014$), and *Actinobacteriota* (0.33% *vs.* 0.11%, $P = 0.002$)

significantly decreased in the PC group. Compared with the PC group, the relative abundance of *Bacteroidota* (66.299% *vs.* 46.4%, $P = 0.003$), *Fusobacteriata* (0.05% *vs.* 0.01%. $P = 0.002$), and *Cyanobacterium* ($P = 0.002$) were significantly lower, while the relative abundances of *Firmicutes* (23.47% *vs.* 42.65%, $P = 0.002$), *Campilobacterota* (0.94% *vs.* 5.03%, $P = 0.04$), and *Patescibactera* ($P = 0.025$) were considerably higher in the AKK group. The ratio of *Firmicutes/Bacteroidotas* (F/B) in the PS group was lower than that in the NC group, as shown in Fig. 4A ($P > 0.05$). The decrease in the ratio of F/B has been
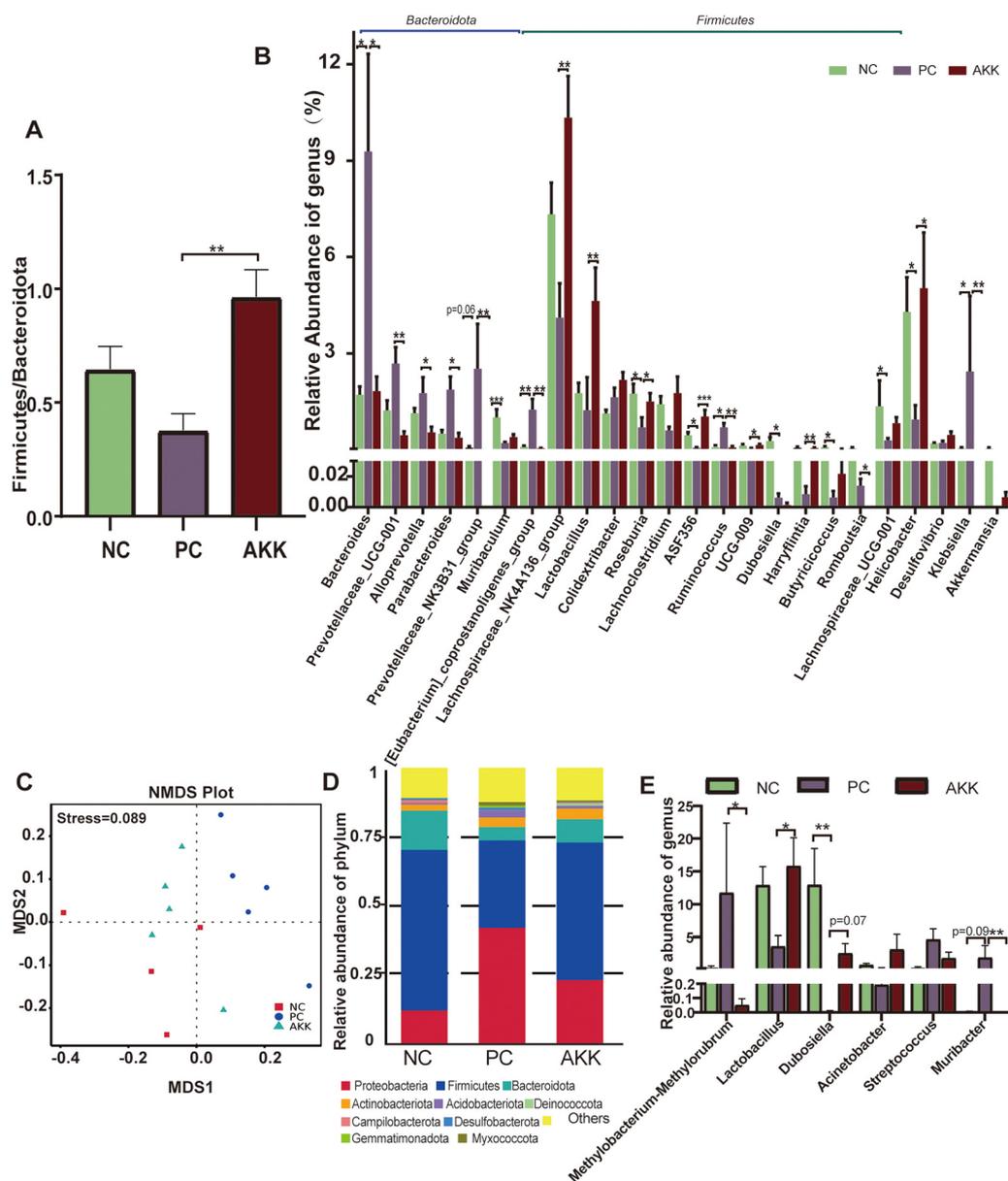

Fig. 4 *A. muciniphila* reshaped the lung and the gut microbiota of mice. (A) There was a significant difference in the *Firmicutes/Bacteroidetes* ratio between the AKK and PC groups ($p < 0.05$). (B) Comparisons of the relative abundances of intestinal microbiota between the three groups were performed at the genus levels ($n = 8$ each group). (C) A NMDS based on weighted Unifrac dissimilarity analysis showed clear separation of the groups ($p < 0.05$), with a stress value of 0.089. Comparisons of the relative abundances of lung microbiota between the three groups were conducted at the phylum (D) and genus (E) level ($n = 4–5$ each group). Data are shown as the mean ± SEM. Compared with the PC group, *$p < 0.05$, **$p < 0.01$, and ***$p < 0.001$. NC, PBS + saline group; PC, PBS + LPS group; AKK, *A. muciniphila* + LPS group.

reported to be linked to inflammation. After AKK intervention treatment, the F/B ratio significantly increased (0.96 vs. 0.37, P = 0.001). At the genus level, the relative abundances of 53 genera ($P < 0.05$) were significantly different in the top 120 genera among the three groups. As shown in Fig. 4B, compared with the NC group, the relative abundances of *Bacteroides*, *Ruminococcus*, [*Eubacterium*]_coprostanoligenes_group and *Klebsiella* were observed to increase, while those of *Muribaculum*, *Lachnospiraceae*_UCG-001, *Roseburia*, ASF356, *Dubosella*, *Butyricicoccus*, and *Helicobacter* decreased in the PC group. Compared with the PC group, the relative abundances of *Lachnospiraceae*_NK4A136_group, *Lactobacillus*, *Roseburia*, ASF356, UCG-009, *Harryflintia* and *Helicobacter* were increased in the AKK group. Additionally, the relative abundances of *Bacteroides*, *Prevotellaceae*_UCG-001, *Alloprevotella*, *Parabacteroides*, *Romboutsia*, *Ruminococcus*, *Prevotellaceae*_NK3B31_group, *Klebsiella* and [*Eubacterium*]_coprostanoligenes_group decreased in the AKK group. As expected, the *Akkermansia* genus was almost completely depleted in the PC group, while there was a tendency of increased levels in the AKK group. Quantitative PCR performed using on fecal DNA revealed that *A. muciniphila*-treated mice had higher levels of *A. muciniphila* than mice in the PC and NC groups ($P < 0.001$), which was presented in ESI Fig. 3.† Overall, the gut microbiota of the lung injury mice was disrupted. Through intervention, the gut microbiota could be reconstructed with differences in the enriched bacterial genera, especially a decrease in the microbes closely related to the production of SCFAs.

A. muciniphila reshaped the lung microbiota of mice

Furthermore, to analyze the relationship between lung microbiota alterations and the lung injury induced by LPS, we conducted 16S rDNA analysis to evaluate the diversity of microflora in the NC ($n = 4$), PC ($n = 5$) and AKK ($n = 5$) groups. No difference was observed in the Chao1, good's coverage, observed OTUs, Shannon and Simpson indexes among the three groups. NMDS based on weighted Unifrac dissimilarity analysis showed clear separation of the groups (Anosim, NC vs. PC, $P = 0.01$; AKK vs. PC, $R = 0.84$, $P = 0.01$), with a stress value of 0.089 (Fig. 4C). At the phylum level (Fig. 4D), the 5 most dominant phyla were *Proteobacteria*, *Firmicutes*, *Bacteroidota*, *Actinobacteriota*, and *Acidobacteriota* in the three groups. At the genus level, the relative abundances of *Lactobacillus* and *Dubosiella* showed an increasing trend ($P < 0.05$), while *Methylobacterium–Methylorubrum* and *Muribacter* levels were significantly lower in the AKK group than in the PC group (Fig. 4E). Using LEfSe analysis, the differences in the lung microbiota composition were identified. According to the results (LDA score >4), the *Firmicutes* phylum, *Erysipelotrichaceae* family, and genera including *Muribaculaceae* and *Dubosiella* were enriched in the NC group, while the *Proteobacteria* phyla, family members belonging to *Streptococcaceae*, *Planococcaceae*, and *Pasteurellaceae*, and genera including *Streptococcus* and *Muribacter* were enriched in the PC group (ESI Fig. 4A†). Additionally, for the *Firmicutes* phyla, families including *Lactobacillaceae*, *Moraxellaceae*, and *Erysipelotrichaceae*, and

genera including *Lactobacillus*, *Acinetobacter*, and *Dubosiella* were enriched in the AKK group. However, for the *Proteobacteria* phyla, genus members including *Muribacter* and *Methylobacterium_Methylorubrum* were enriched in the PC group (ESI Fig. 4B†). In summary, we concluded that the ecological balance of the lung microbiota was disrupted in lung-injured mice and that *A. muciniphila* reshaped the lung microbiota.

To investigate the relationship between pulmonary microbiota and intestinal microbiota, a Spearman correlation analysis was performed (ESI Fig. 5†). The presence of *Muribacter* in the lungs of the PC group exhibited a positive correlation with the relative abundances of various intestinal members, including *Bacteroides*, *Prevotellaceae_UCG-001*, *Klebsiella*, *Alloprevotella*, *Parabacteroides*, and *Prevotellaceae_NK3B31_* group ($P < 0.05$). Conversely, the presence of *Dubosella* in the lungs of the AKK group showed a negative association with intestinal *Bacteroides*, *Prevotellaceae_UCG-001*, and *Klebsiella* ($P < 0.05$). The presence of *Lactobacillus*, which was found to be more abundant in the lungs of the AKK group, exhibited a positive correlation with the intestinal *Lachnospiraceae_NK4A136*_group, *Lachnospiraceae_UCG-001*, and [*Eubacterium*]_*xylanophilum*_group ($P < 0.05$). Meanwhile, it showed a negative correlation with *Klebsiella* in the intestine ($P < 0.05$). These findings indicated that the manipulation of the gut microbiota through probiotics maybe lead to alterations in the composition of the host lung microbiota.

A. muciniphila promoted the production of SCFAs by regulating the gut microbiota

SCFAs are only produced by microbial fermentation in the host. First, we conducted a targeted metabolomics analysis to measure the concentration of specific SCFAs (acetic acid, propionic acid, isovaleric acid, butyric acid, isobutyric acid, and valeric acid) in colonic contents (Fig. 5). Compared with the NC group, the LPS intervention significantly reduced the concentrations of isobutyric acid and isovaleric acid ($P < 0.05$), and the concentrations of propionic acid, valeric acid, and acetic acid showed a downward trend. Compared with the PC group, the levels of acetic acid, propionic acid, isovaleric acid, butyric acid, isobutyric acid, and valeric acid in the AKK group notably increased ($P < 0.05$), indicating that *A. muciniphila* can promote the synthesis of SCFAs by the gut microbiota.

A. muciniphila regulated lung transcriptional expression in LPS-induced lung injury

To explore the important role of *A. muciniphila* in improving LPS-induced lung injury in mice, we conducted a transcriptome analysis of lung tissues harvested from the PC ($n = 4$), NC ($n = 3$) and AKK ($n = 3$) groups. As shown in ESI Fig. 6,† there were a total of 13 395 genes in the three groups and 351 genes in the AKK and PC groups. The above results suggested that the three groups had significantly different gene expression patterns. The standard for differential genes was that the absolute value of the log2-fold change was greater than 1, and the P value was less than 0.05. Among these differentially expressed genes (DEGs), 1687 and 1195 DEGs were signifi-
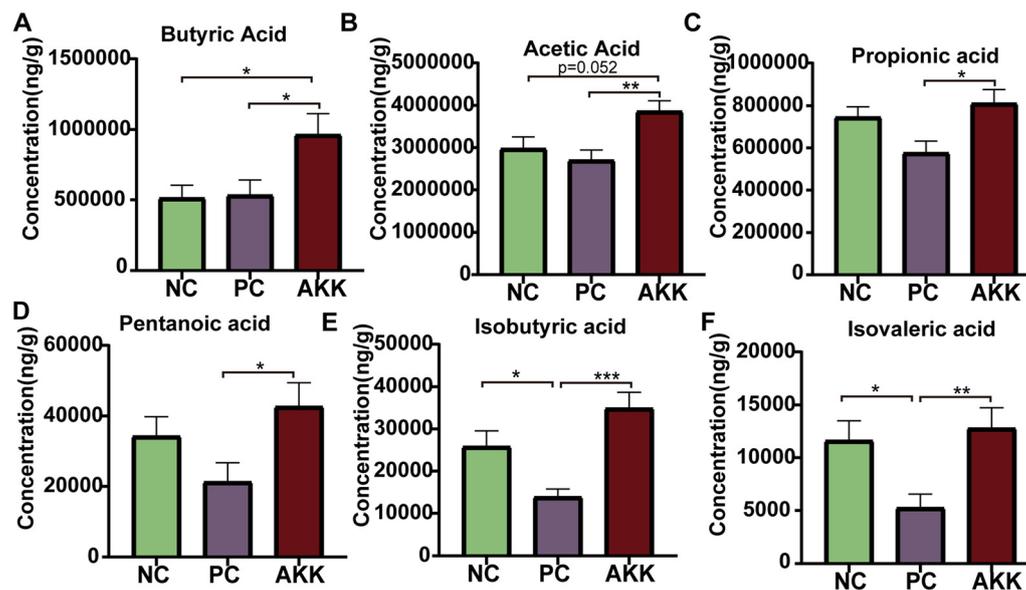
Fig. 5 *A. muciniphila* regulates intestinal microbiota to promote the production of SCFAs. The concentration of short-chain fatty acids in feces, mainly included butyric acid (A), acetic acid (B), propionic acid (C), pentanoic acid (D), isobutyric acid (E), and isovaleric acid (F). All data are expressed as the mean ± SEM; * represents $p < 0.05$, ** represents $p < 0.01$, and *** represents $p < 0.001$. NC, PBS + saline group; PC, PBS + LPS group; AKK, *A. muciniphila* + LPS group. $n = 8$ each group.

cantly upregulated and downregulated in the PC group compared to the NC group, respectively. In comparison with the PC group, 234 and 561 DEGs were significantly upregulated and downregulated in the AKK group, respectively. Furthermore, we mapped these genes to the KEGG pathway database, and focused on overlapping pathways in the analysis. Finally, 59 meaningfully inhibited pathways were identified, determined by an adj-$P < 0.05$. In the top 20 pathways, the immune response (toll-like receptor signalling pathway, NOD-like receptor signalling pathway, osteoclast differentiation and cytokine–cytokine receptor interaction), NF-kappa B signalling pathway, and infection (Epstein–Barr virus infection, herpes simplex infection, Legionellosis, Leishmaniasis, Malaria, Pertussis, *Salmonella* infection, *Staphylococcus aureus* infection and tuberculosis) were induced by *A. muciniphila* (Figure 6B). Protein–protein interaction (PPI) networks were constructed by mapping genes from the significantly inhibited pathways to classify genes involved in lung protection. The key gene network was explored using the cluster containing the highest MCODE score (Table S3†) on the PPI network after it was formed, using MCODE of Cytoscape 3.10.0. The key hub genes were as follows: TLR4, TLR2, chemokine ligand (Cxcl9, Ccl2, Ccl20, Ccl4, Ccl9, Ccr1, Cxcl1, Cxcl13, Cxcl2, Cxcl3, Cxcl5, Cxcl9), IL1b, IL12b, NCf2, NF-kB and others (Fig. 6C). Undoubtedly, a close relationship existed between the lung injury progression and inflammation.

A. muciniphila-induced antioxidant activity and inflammation

As LPS induces ALI, oxidative stress plays a considerable role. MDA is a common product of lipid peroxidation, and SOD is one of the most effective antioxidant enzymes for scavenging superoxide anion free radicals. MDA and SOD concentrations in lung tissues were measured to assess the oxidative stress markers. In comparison with the NC group, the MDA concentration in lung tissue increased significantly ($P = 0.005$) after LPS modelling, while the MDA concentration significantly decreased ($P = 0.02$) after AKK intervention (Fig. 6D). Additionally, compared with the NC group, the SOD activity (SOD expressed as inhibition rate %) in the lung was significantly reduced in the PC group ($P < 0.001$), while AKK induced an increase ($P < 0.001$) (Fig. 6E). LPS enhanced the oxidative stress response, and probiotic intervention alleviated the response by inhibiting the MDA level and improving the SOD activity. The above results suggest that oxidative stress plays an important role in the progression of the lung injury.

Additionally, TLRs and NF-kB signalling pathways contribute significantly to inflammation. Accompanied with the NC group, the mRNA expression levels of TLR2 ($P < 0.001$), TLR5 ($P < 0.01$), MYD88 ($P < 0.01$), and NF-kB ($P < 0.001$) were significantly increased in the PC group, while *A. muciniphila* intervention remarkably reduced TLR2 ($P < 0.001$), MYD88 ($P < 0.01$), and NF-kB expression ($P < 0.01$) (Fig. 6F). Based on these results, *A. muciniphila* improved the inflammatory microenvironment by suppressing the TLRs expression, which led to the inhibition of NF-kB-mediated inflammation.

Butyrate supplementation alleviated LPS-induced lung injury

A. muciniphila can ameliorate LPS-induced lung injury in mice by promoting the secretion of SCFAs, and the SCFAs result in our study showed that the most significant increase in the AKK group is butyric acid. To further investigate the protective effect of SCFAs, we explored whether butyrate supplementation
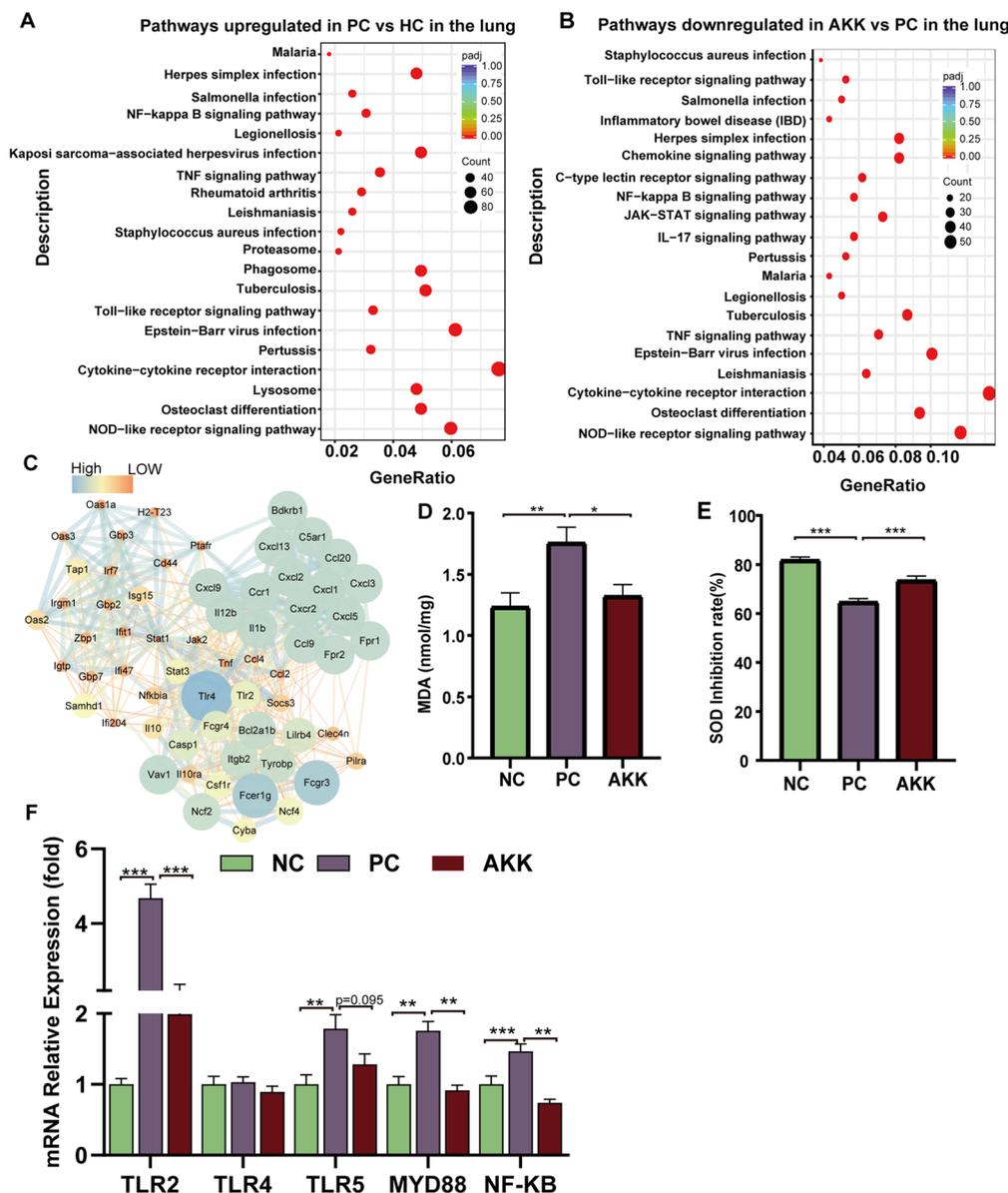
Fig. 6 The effect of *A. muciniphila* treatment on mouse lung transcriptome and its improvement in antioxidant activity and inflammation. (A) Pathways were upregulated by LPS stimulation; (B) pathways were downregulated by *A. muciniphila* treatment in the lung (n = 3–4 each group). (C) Visualization of the cluster network with the highest MCODE score. The concentration of MDA (D) and SOD inhibition (E) in lung tissue was measured by ELISA (n = 8 each group). (F) Relative lung mRNA expression (TLR2, TLR4, TLR5, MYD88 and NF-kappa b). Target gene expression levels were normalized using β-actin levels. All data are shown as the mean ± SEM; * represents $p < 0.05$, ** represents $p < 0.01$, and *** represents $p < 0.001$. NC, PBS + saline group; PC, PBS + LPS group; AKK, *A. muciniphila* + LPS group.

could ameliorate LPS-induced lung injury. We divided the mice into 4 groups: NC (water + saline) group, NCB (butyric acid + saline) group, LPS (PBS + LPS) group, and BAL (butyric acid + LPS) group. The mice in the NCB and B groups were supplemented with butyric acid (100 mM, Sigma, B103500, USA) containing drinking water for 21 days, with fresh butyric acid solution configured every 3 days, and the NC and LPS groups received regular drinking water. On day 22, the LPS and B group mice received ALI modelling consistently as before, while the NCB and NC group mice were given the same volume of saline as shown in Fig. 7A. Interestingly, butyric

acid supplementation significantly improved the body weight (Fig. 7B), W/D ratio (Fig. 7C) and degree of lung fibrosis (Fig. 7J) in the BAL group mice compared to those with the LPS group. In addition, butyric acid intervention improved the integrity of the alveolar barrier, as shown in Fig. 7D–F. We measured the total protein levels, total cell counts, and LDH activity in BALF, and the above indexes were significantly reduced on mice in the BAL group ($P < 0.05$). Meanwhile, butyric acid treatment improved the inflammatory response on mice in the BAL group. As shown in Fig. 7G and H, the levels of IL-1β ($P < 0.01$) and IL-6 ($P < 0.001$) in alveolar lavage fluid
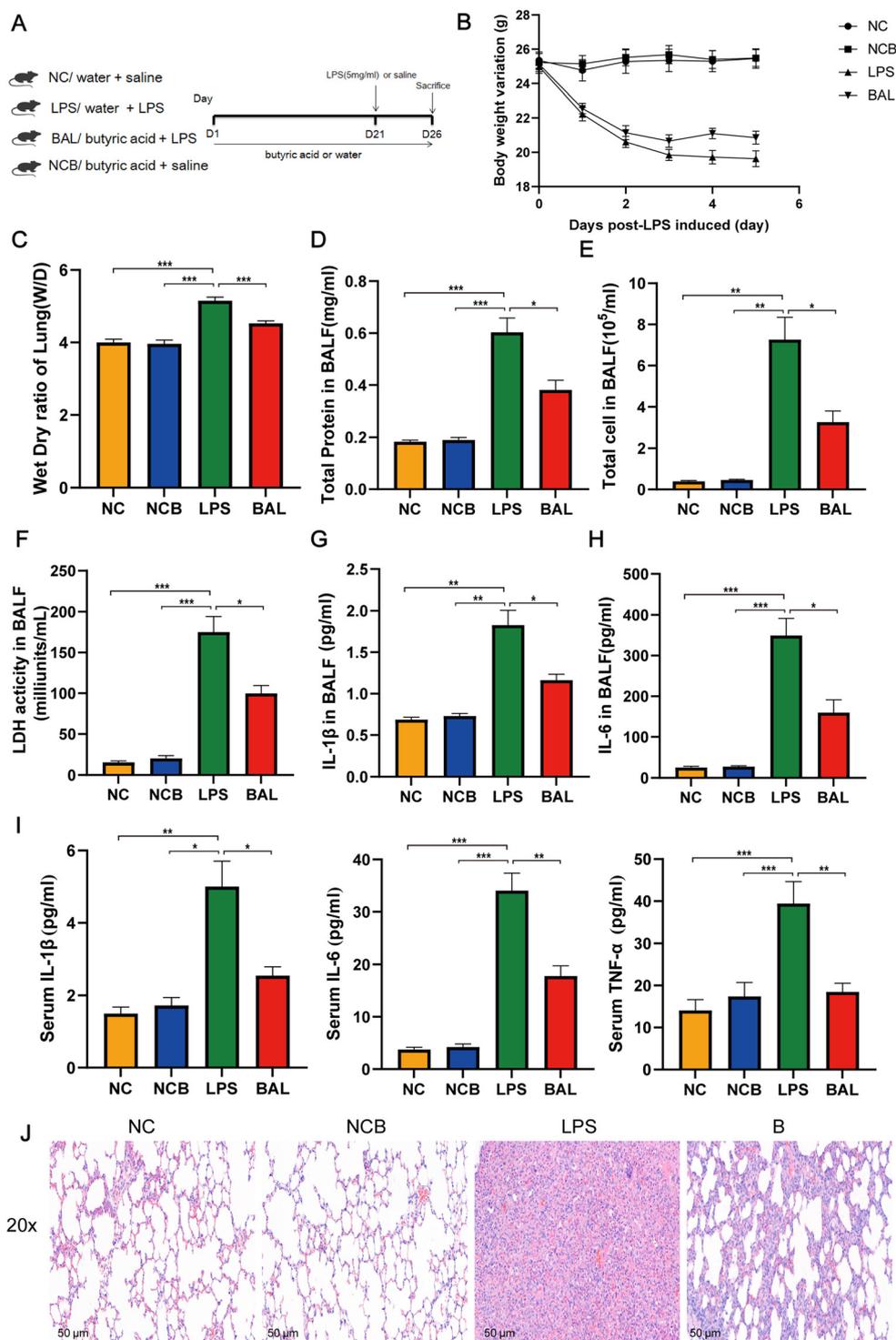
Fig. 7 Butyrate supplementation alleviated LPS-induced lung injury. Experimental flowchart (A); changes in body weight (B) and lung dry wet ratio in mice (C); concentration of total protein (D), total cell count (E), and LDH activity (F) in BALF; IL-1β (G) and IL-6 (H) levels in BALF; (I) serum levels of IL-1β, IL-6, and TNF-α; (J) representative images of HE staining in lung tissue (scale = 50 μm); data are presented as the mean ± SEM; compared with the LPS group, *$p < 0.05$, **$p < 0.01$, and ***$p < 0.001$. NC, water + saline group; LPS, water + LPS group; BAL, butyric acid + LPS group; NCB, butyric acid + saline group; $n = 8$ each group. BALF, bronchoalveolar lavage fluid.

were elevated in the LPS group, whereas the levels of the above factors were much lower in the BAL group than in the LPS group ($P < 0.05$). In addition, butyric acid intervention improved the levels of serum pro-inflammatory factors IL-1β, IL-6 and TNF-α (Fig. 7I) ($P < 0.05$). We also found that butyric acid supplementation would have no effect on mice in the NC

group ($P > 0.05$). These results suggest that lung oedema and alveolar epithelial permeability can be improved with butyrate supplementation, and pulmonary and systemic inflammatory response.

Furthermore, Fig. 8A shows that the administration of butyric acid through drinking water resulted in an increase in the concentration of cecum butyric acid. The LEfSe method was employed to examine the significant changes in key phylo-
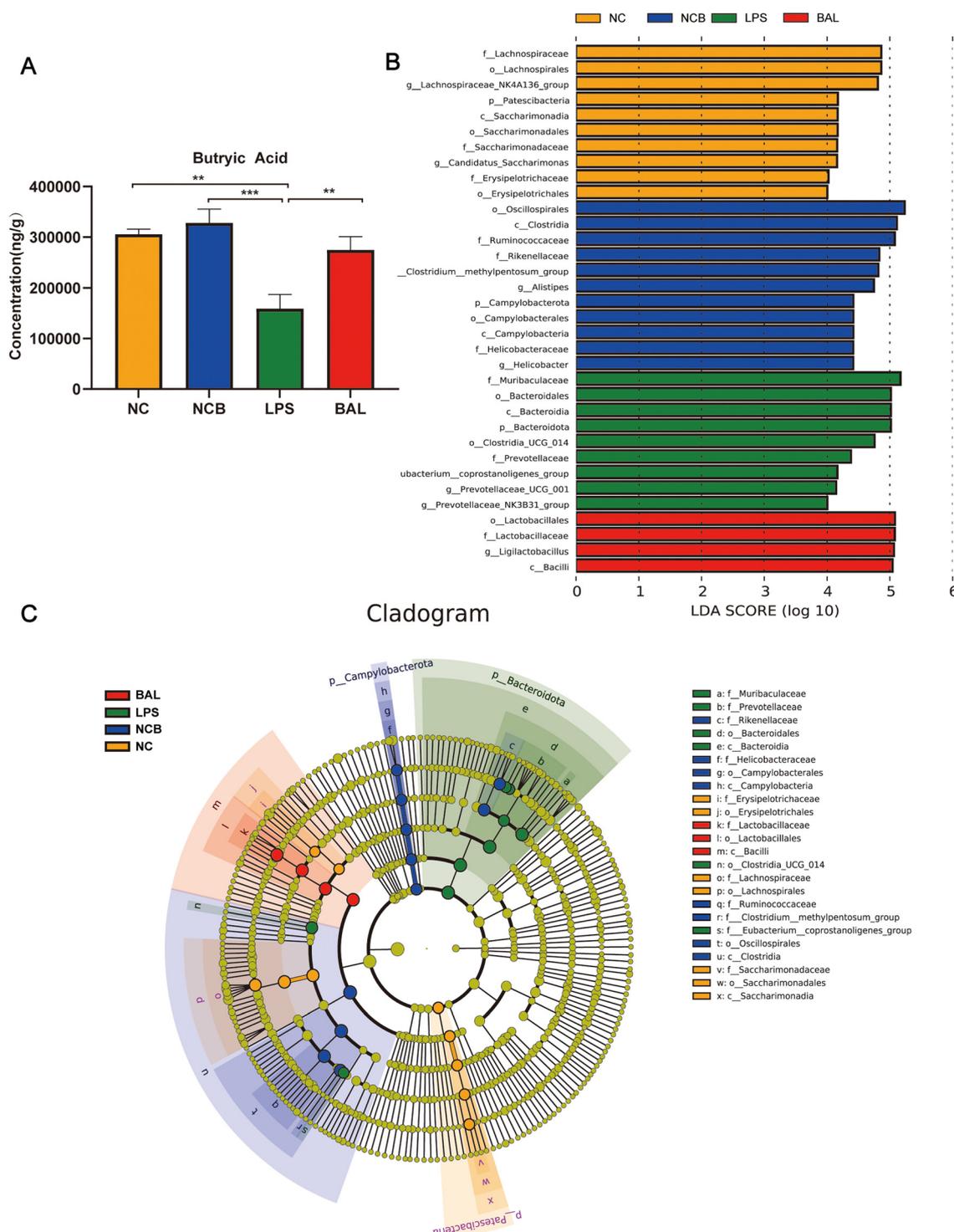

Fig. 8 Effect of butyrate supplementation on the gut microbiota of mice. (A) The concentration of butyric acid in cecum contents. (B) LEfSe analyses identified the differentially abundant taxa between the four groups. (C) The differential species branching diagram between the four groups. Data are presented as the mean ± SEM; compared with the LPS group, *$p < 0.05$, **$p < 0.01$, and ***$p < 0.001$. NC, water + saline group; LPS, water + LPS group; BAL, butyric acid + LPS group; NCB, butyric acid + saline group; $n = 8$ each group. LEfSe, linear discriminant analysis effect size.

genetic types following butyric acid treatment, using an LDA threshold greater than 4. The NC group exhibited enrichment of the genus of *Lachnospiraceae*_NK4A136_group and *Candidatus_Saccharimonas*, while the LPS group showed enrichment of the genus *Prevotellaceae*_UCG_001 and *Eubacterium_Coprostanogenes*_group. The BAL group demonstrated enrichment of the genus *Ligilactobacillius*, and the NCB group exhibited enrichment of the family *Ruminococcaceae*, genus *Helicobacter*, *Alistipe*s and *Prevotelaceae*_NK3B31_group (Fig. 8B). These findings suggested that butyric acid did not completely alter the structure of the gut microbiota, but rather increases the abundance of probiotics in ALI mice.

Discussion

Numerous studies have indicated that disorders of the gut[25] and lung[26] microbiota exacerbate ALI, which is attributed to the microbiota and its metabolic byproducts.[27] Moreover, the main direction of crosstalk is from the gut to the lungs, but it is still possible for communication to occur in the opposite direction.[27] *A. muciniphila* is also known to have high anti-inflammatory and antioxidative stress properties, and promote colonization of the colon by SCFA-producing bacteria in mice.[28] Multiple research studies have found that *A. muciniphila* plays an important role in numerous diseases, such as liver steatosis, obesity, cancer immunotherapy, and gut barrier and intestinal inflammation.[29] There is insufficient evidence to determine whether *A. muciniphila* is protective against ALI. Our research showed that *A. muciniphila* administration significantly attenuated LPS-induced ALI by reducing serum LBP levels, regulating lung oxidative stress, and alleviating lung inflammation partly by remodeling the composition of the gut microbiota and increasing the colonic butyrate concentrations. In this context, the use of probiotics might represent a useful strategy for maintaining the balance of the gut microbiota and inhibiting lung inflammation to improve ALI.

Unquestionably, inflammation has a critical effect on ALI/ARDS, which can directly or indirectly lead to damage to the alveolar epithelium and pulmonary microvascular endothelium, even increasing microvascular permeability, and resulting in refractory hypoxemia.[30,31] Thus, inflammatory cell influx, cytokine release, and protein leakage are key events in ALI.[32,33] Surprisingly, we discovered that *A. muciniphila* decreased the levels of inflammatory mediators and improved permeabilization of the alveolocapillary barrier. Our findings were consistent with the finding that inhibiting inflammation contributed to mitigation of pulmonary tissue injury.[25,33] Local tissue injury and microbial infection activate immunologic cells, which produce inflammatory cytokines, such as IL-1β and IL-6, causing more severe mucosal injury.[34] IL-6 was reported to drive the differentiation of Th17 cells by activating STAT3, thereby enhancing neutrophil recruitment and reducing the bacterial burden.[35] Our study revealed key hub genes, including TLR4, TLR2, chemokine ligand, and NF-kB, in the transcriptome analysis. Toll-like receptors (such as TLR4/TLR2, *etc*.) expressed on immune cells (especially macrophages) activate the immune system and inflammation, driving lung injury, which participates in the loss of the barrier integrity and bacterial translocation.[36,37] Multiple lung cells, including macrophages, DCs, and activated endothelial and vascular smooth muscle cells have been shown to highly express TLR2.[38–40] Our results suggested that AKK significantly reduced the expression of TLR2 and TLR5, but not TLR4. Following attachment to LBP, LPS toll-like receptors mediate inflammatory reactions.[41] In the LPS-induced ALI model, TLR2/Myd88/NF-κB activation (p65 subunit phosphorylation) induces MCP-1, TNF-α, IL-6, and IL-1β secretion.[42,43] The inhibited LBP played a vital role in reducing the expression of pro-inflammatory factors.[44] To a certain extent, modifying the gut microbiota can reduce the levels of serum pro-inflammatory factors and LPS, and play a role in the prevention and treatment of ALL.[41] Additionally, we observed that *A. muciniphila* increased the expression of intestinal ZO-1 and occludin, as well as the production of SCFAs, indicating that its anti-inflammatory properties are closely related to the repair of damaged intestinal barrier function, which is consistent with previous reports.[45]

In ALI, lung oxidative stress and inflammation cause cellular damage.[46] After LPS stimulation, the level of antioxidant stress in the lungs was significantly reduced, which was characterized by a decrease in SOD activity and MDA levels. This is consistent with previous research reports, and suggests a close relationship between oxidative stress and ALI.[47] As a natural antioxidant, SOD scavenged free radicals, which was treated as a vital defense mechanism.[48] Measurement of lipid peroxidation is usually based on MDA, the end product of lipid peroxidation.[49] Our study showed a significant decrease in MDA levels and an increase in SOD activity in the AKK group, which was a marker of alleviation of the lung oxidative stress response. This may be attributed to the reshaping of the bacterial community structure and a decrease in intestine-derived LPS levels. *A. muciniphila* significantly reduced LBP levels, may have blocked the production of reactive oxygen species induced by LPS, and even alleviated inflammatory reactions. Previously published data support this conclusion.[50]

Accumulating studies have investigated the roles of gut–lung axis and treatment with prebiotics in lung disease.[51,52] As noted in the literature, *A. muciniphila* has been found to improve LPS-induced lung injury.[51,53] *A. muciniphila* induced significant improvement in both the F/B ratio and the relative abundance of *A. muciniphila* in our study. Moreover, this study found that *Klebsiella* was enriched in animals with LPS-induced ALI. *Klebsiella* proliferate abnormally and colonize the gut, aggravating the inflammation in inflammatory bowel disease.[54] Interestingly, well-known SCFA-producing bacteria, including *Lachnospiraceae*_NK4A136_group,[55] *Lactobacillus*,[56] *Roseburia*,[57] and ASF356,[58] are inversely related to systemic inflammation. In addition, we found that treatment with *A. muciniphila* caused a significant elevation in the levels of SCFAs, such as acetic acid, propionic acid, isovaleric acid, butyric acid, isobutyric acid, and valeric acid. Butyrate and

acetate are helpful for intestinal function in a variety of ways, including improving the intestinal barrier, improving the microbiota in the intestine, regulating the immune system, and promoting gastrointestinal motility.[57] Furthermore, propionic acid significantly inhibited the production of pro-inflammatory cytokines, while enhancing the production of anti-inflammatory cytokines.[59] Butyrate has been extensively identified as an inhibitor of the HDAC enzyme that alleviates lung injury by suppressing the expression of NF-κB p65.[60] Based on these results, it is hypothesized that *A. muciniphila* rebuilds the intestinal flora structure and promotes SCFA production, which is necessary for mitigating the pathological features of lung damage.

Furthermore, the administration of butyrate as a supplement demonstrated notable protective effects, leading to a significant enhancement in the integrity of the alveolar barrier. This subsequently resulted in a reduction in both pulmonary and systemic inflammatory reactions, as evidenced by the decreased levels of pro-inflammatory factors, such as IL-1β, IL-6, and TNF-α. Additionally, the provision of energy to colon cells through butyrate supplementation effectively safeguarded the intestinal mucosa against the infiltration of bacteria into the bloodstream, thereby mitigating the initiation of inflammatory responses. This finding is supported by previous research.[61] The study provides undeniable evidence that the supplementation of butyrate significantly enhances the presence of *Ligilactobacillius*, a well-regarded probiotic.[62] This finding aligns with previous research that suggests an increase in *Proteobacterium* abundance in the intestine is indicative of an unstable microbial community, serving as a crucial indicator for assessing gut microbiota disorders.[63] Overall, the observed disappearance of the regulatory effect of butyrate on the gut microbiota of ALI mice suggests that the adjustment of intestinal microbiota in these mice is challenging.

Numerous studies have shown that the microbiome in the respiratory tract contributes to a variety of lung diseases, such as idiopathic pulmonary fibrosis, asthma and lung cancer.[64] Recent studies have examined whether ALI is correlated with a change in the gut microbiota,[51,53] but few have investigated the difference in the lung microbiota in lung injury. Composition analysis of the lung microbiota showed that the abundance of *Firmicutes* significantly increased after treatment, while *Proteobacteria* abundance significantly increased after LPS exposure in our study. Lung flora disturbance in numerous lung diseases was characterized by the increased relative abundance of *Proteobacteria*, while the abundance of *Firmicutes* decreased.[65] After acute stress, the excessive production of pro-inflammatory cytokines leads to higher levels of ROS and reactive nitrogen, further resulting in the accumulation of nitrate in lung tissue, with pathogens (such as *Pseudomonas aeruginosa*) thriving at sites of inflammation.[66,67] *Firmicutes*, including *Erysipelotrichaceae* and *Lactobacillaceae*, are butyrate-producing taxa,[68] which may be related to the modulation of the microbiota composition.

Generally, our results indicated that the microbiota, including that of the colon and lung tissue, may be a key factor in the development of inflammation and oxidative stress in LPS-induced pulmonary tissue and provided evidence that damaged microbiota may affect pulmonary inflammation and oxidative stress during LPS exposure. We also observed that *A. muciniphila* repaired the damaged intestinal barrier, which was related to the remodeling of the gut microbiota and the enhancement of SCFA secretion. The butyric acid supplementation experiment further confirmed the efficacy of *A. muciniphila* in reducing ALI, led by changes in intestinal butyric acid concentration. This study provided a deeper understanding of the underlying mechanisms of lung inflammation and oxidative stress during LPS exposure, and indicated that *A. muciniphila* had a positive impact on lung inflammation and oxidative damage.

Ethics statement

All animal procedures were performed in accordance with the Guidelines for Care and Use of Laboratory Animals of Zhejiang University, and approved by the Animal Ethics Committee of Animal Experiments (Zhejiang, China) of the First Affiliated Hospital of Zhejiang University (2023-969).

Data availability

Lung and feces 16S rRNA data and liver transcriptome date have been transmitted to the sequence read archive (PRJNA992760, PRJNA992679 and PRJNA992927).

Author contributions

Lanjuan Li, Jian Shen, and Shuting Wang contributed to the study conception and design. Material preparation, data collection and analysis were performed by Jian Shen, Shuting Wang, He Xia, Shenyi Han, Qiangqiang Wang, Zhengjie Wu, Aoxiang Zhug, Shengjie Li and Hui Chen. The first draft of the manuscript was written by Jian Shen, and all authors commented on previous versions of the manuscript. All authors read and approved the final manuscript.

Conflicts of interest

We have no competing interests to declare in this study.

Acknowledgements

Jinan Microecological Biomedicine Shandong Laboratory (JNL-2022045D).

References

1 J. L. Mendez and R. D. Hubmayr, New insights into the pathology of acute respiratory failure, *Curr. Opin. Crit. Care*, 2005, **11**, 29–36.

2 S. Haga, N. Yamamoto, C. Nakai-Murakami, Y. Osawa, K. Tokunaga, T. Sata, N. Yamamoto, T. Sasazuki and Y. Ishizaka, Modulation of TNF-alpha-converting enzyme by the spike protein of SARS-CoV and ACE2 induces TNF-alpha production and facilitates viral entry, *Proc. Natl. Acad. Sci. U. S. A.*, 2008, **105**, 7809–7814.

3 N. J. Meyer, L. Gattinoni and C. S. Calfee, Acute respiratory distress syndrome, *Lancet*, 2021, **398**, 622–637.

4 Y. Zhou, P. Li, A. J. Goodwin, J. A. Cook, P. V. Halushka, E. Chang, B. Zingarelli and H. Fan, Exosomes from endothelial progenitor cells improve outcomes of the lipopolysaccharide-induced acute lung injury, *Crit. Care*, 2019, **23**, 44.

5 T. Takagi, O. Taguchi, S. Aoki, M. Toda, A. Yamaguchi, H. Fujimoto, D. Boveda-Ruiz, P. Gil-Bernabe, A. Y. Ramirez, M. Naito, Y. Yano, C. N. D'Alessandro-Gabazza, A. Fujiwara, Y. Takei, J. Morser and E. C. Gabazza, Direct effects of protein S in ameliorating acute lung injury, *J. Thromb. Haemostasis*, 2009, **7**, 2053–2063.

6 S. R. Lewis, M. W. Pritchard, C. M. Thomas and A. F. Smith, Pharmacological agents for adults with acute respiratory distress syndrome, *Cochrane Database Syst. Rev.*, 2019, **7**, Cd004477.

7 Y. K. Yeoh, T. Zuo, G. C. Lui, F. Zhang, Q. Liu, A. Y. Li, A. C. Chung, C. P. Cheung, E. Y. Tso, K. S. Fung, V. Chan, L. Ling, G. Joynt, D. S. Hui, K. M. Chow, S. S. S. Ng, T. C. Li, R. W. Ng, T. C. Yip, G. L. Wong, F. K. Chan, C. K. Wong, P. K. Chan and S. C. Ng, Gut microbiota composition reflects disease severity and dysfunctional immune responses in patients with COVID-19, *Gut*, 2021, **70**, 698–706.

8 P. Gutierrez-Castrellon, T. Gandara-Marti, Y. A. A. T. Abreu, C. D. Nieto-Rufino, E. Lopez-Orduna, I. Jimenez-Escobar, C. Jimenez-Gutierrez, G. Lopez-Velazquez and J. Espadaler-Mazo, Probiotic improves symptomatic and viral clearance in Covid19 outpatients: a randomized, quadruple-blinded, placebo-controlled trial, *Gut Microbes*, 2022, **14**, 2018899.

9 V. Ivashkin, V. Fomin, S. Moiseev, M. Brovko, R. Maslennikov, A. Ulyanin, V. Sholomova, M. Vasilyeva, E. Trush, O. Shifrin and E. Poluektova, Efficacy of a Probiotic Consisting of Lacticaseibacillus rhamnosus PDV 1705, Bifidobacterium bifidum PDV 0903, Bifidobacterium longum subsp. infantis PDV 1911, and Bifidobacterium longum subsp. longum PDV 2301 in the Treatment of Hospitalized Patients with COVID-19: a Randomized Controlled Trial, *Probiotics Antimicrob. Proteins*, 2021, 1–9, DOI: 10.1007/s12602-021-09858-5.

10 C. Wu, Q. Xu, Z. Cao, D. Pan, Y. Zhu, S. Wang, D. Liu, Z. Song, W. Jiang, Y. Ruan, Y. Huang, N. Qin, H. Lu and H. Qin, The volatile and heterogeneous gut microbiota shifts of COVID-19 patients over the course of a probiotics-assisted therapy, *Clin. Transl. Med.*, 2021, **11**, e643.

11 X. Jin, J. S. Lian, J. H. Hu, J. Gao, L. Zheng, Y. M. Zhang, S. R. Hao, H. Y. Jia, H. Cai, X. L. Zhang, G. D. Yu, K. J. Xu, X. Y. Wang, J. Q. Gu, S. Y. Zhang, C. Y. Ye, C. L. Jin, Y. F. Lu, X. Yu, X. P. Yu, J. R. Huang, K. L. Xu, Q. Ni, C. B. Yu, B. Zhu, Y. T. Li, J. Liu, H. Zhao, X. Zhang, L. Yu, Y. Z. Guo, J. W. Su, J. J. Tao, G. J. Lang, X. X. Wu, W. R. Wu, T. T. Qv, D. R. Xiang, P. Yi, D. Shi, Y. Chen, Y. Ren, Y. Q. Qiu, L. J. Li, J. Sheng and Y. Yang, Epidemiological, clinical and virological characteristics of 74 cases of coronavirus-infected disease 2019 (COVID-19) with gastrointestinal symptoms, *Gut*, 2020, **69**, 1002–1009.

12 Z. Ren, H. Wang, G. Cui, H. Lu, L. Wang, H. Luo, X. Chen, H. Ren, R. Sun, W. Liu, X. Liu, C. Liu, A. Li, X. Wang, B. Rao, C. Yuan, H. Zhang, J. Sun, X. Chen, B. Li, C. Hu, Z. Wu, Z. Yu, Q. Kan and L. Li, Alterations in the human oral and gut microbiomes and lipidomics in COVID-19, *Gut*, 2021, **70**, 1253–1265.

13 S. Gu, Y. Chen, Z. Wu, Y. Chen, H. Gao, L. Lv, F. Guo, X. Zhang, R. Luo, C. Huang, H. Lu, B. Zheng, J. Zhang, R. Yan, H. Zhang, H. Jiang, Q. Xu, J. Guo, Y. Gong, L. Tang and L. Li, Alterations of the Gut Microbiota in Patients With Coronavirus Disease 2019 or H1N1 Influenza, *Clin. Infect. Dis*, 2020, **71**, 2669–2678.

14 F. Zhang, Y. Wan, T. Zuo, Y. K. Yeoh, Q. Liu, L. Zhang, H. Zhan, W. Lu, W. Xu, G. C. Y. Lui, A. Y. L. Li, C. P. Cheung, C. K. Wong, P. K. S. Chan, F. K. L. Chan and S. C. Ng, Prolonged Impairment of Short-Chain Fatty Acid and L-Isoleucine Biosynthesis in Gut Microbiome in Patients With COVID-19, *Gastroenterology*, 2022, **162**, 548–561 e544.

15 Y. H. Wang, Z. Z. Yan, S. D. Luo, J. J. Hu, M. Wu, J. Zhao, W. F. Liu, C. Li and K. X. Liu, Gut microbiota-derived succinate aggravates acute lung injury after intestinal ischaemia/reperfusion in mice, *Eur. Respir. J.*, 2023, **61**, 2200840.

16 R. P. Dickson, M. J. Schultz, T. van der Poll, L. R. Schouten, N. R. Falkowski, J. E. Luth, M. W. Sjoding, C. A. Brown, R. Chanderraj, G. B. Huffnagle and L. D. J. Bos, Lung Microbiota Predict Clinical Outcomes in Critically Ill Patients, *Am. J. Respir. Crit. Care Med.*, 2020, **201**, 555–563.

17 Y. Hashimoto, A. Eguchi, Y. Wei, H. Shinno-Hashimoto, Y. Fujita, T. Ishima, L. Chang, C. Mori, T. Suzuki and K. Hashimoto, Antibiotic-induced microbiome depletion improves LPS-induced acute lung injury via gut-lung axis, *Life Sci.*, 2022, **307**, 120885.

18 T. Zhang, Q. Li, L. Cheng, H. Buch and F. Zhang, Akkermansia muciniphila is a promising probiotic, *Microb. Biotechnol.*, 2019, **12**, 1109–1125.

19 Z. Wu, Q. Xu, S. Gu, Y. Chen, L. Lv, B. Zheng, Q. Wang, K. Wang, S. Wang, J. Xia, L. Yang, X. Bian, X. Jiang, L. Zheng and L. Li, Akkermansia muciniphila Ameliorates Clostridioides difficile Infection in Mice by Modulating the

Intestinal Microbiome and Metabolites, *Front. Microbiol.*, 2022, **13**, 841920.

20 W. Wu, L. Lv, D. Shi, J. Ye, D. Fang, F. Guo, Y. Li, X. He and L. Li, Protective Effect of Akkermansia muciniphila against Immune-Mediated Liver Injury in a Mouse Model, *Front. Microbiol.*, 2017, **8**, 1804.

21 J. Xia, L. Lv, B. Liu, S. Wang, S. Zhang, Z. Wu, L. Yang, X. Bian, Q. Wang, K. Wang, A. Zhuge, S. Li, R. Yan, H. Jiang, K. Xu and L. Li, Akkermansia muciniphila Ameliorates Acetaminophen-Induced Liver Injury by Regulating Gut Microbial Composition and Metabolism, *Microbiol. Spectrum*, 2022, **10**, e0159621.

22 L. Lv, C. Yao, R. Yan, H. Jiang, Q. Wang, K. Wang, S. Ren, S. Jiang, J. Xia, S. Li and Y. Yu, Lactobacillus acidophilus LA14 Alleviates Liver Injury, *mSystems*, 2021, **6**, e0038421.

23 S. D. Wright, R. A. Ramos, P. S. Tobias, R. J. Ulevitch and J. C. Mathison, CD14, a receptor for complexes of lipopolysaccharide (LPS) and LPS binding protein, *Science*, 1990, **249**, 1431–1433.

24 L. B. Giron, H. Dweep, X. Yin, H. Wang, M. Damra, A. R. Goldman, N. Gorman, C. S. Palmer, H. Y. Tang, M. W. Shaikh, C. B. Forsyth, R. A. Balk, N. F. Zilberstein, Q. Liu, A. Kossenkov, A. Keshavarzian, A. Landay and M. Abdel-Mohsen, Plasma Markers of Disrupted Gut Permeability in Severe COVID-19 Patients, *Front. Immunol.*, 2021, **12**, 686240.

25 Y. Xu, J. Zhu, B. Feng, F. Lin, J. Zhou, J. Liu, X. Shi, X. Lu, Q. Pan, J. Yu, Y. Zhang, L. Li and H. Cao, Immunosuppressive effect of mesenchymal stem cells on lung and gut CD8(+) T cells in lipopolysaccharide-induced acute lung injury in mice, *Cell Proliferation*, 2021, **54**, e13028.

26 M. A. Sze, M. Tsuruta, S. W. Yang, Y. Oh, S. F. Man, J. C. Hogg and D. D. Sin, Changes in the bacterial microbiota in gut, blood, and lungs following acute LPS instillation into mice lungs, *PLoS One*, 2014, **9**, e111228.

27 A. T. Dang and B. J. Marsland, Microbes, metabolites, and the gut-lung axis, *Mucosal Immunol.*, 2019, **12**, 843–850.

28 D. J. Warman, H. Jia and H. Kato, The Potential Roles of Probiotics, Resistant Starch, and Resistant Proteins in Ameliorating Inflammation during Aging (Inflammaging), *Nutrients*, 2022, **14**, 747.

29 P. D. Cani, C. Depommier, M. Derrien, A. Everard and W. M. de Vos, Akkermansia muciniphila: paradigm for next-generation beneficial microorganisms, *Nat. Rev. Gastroenterol. Hepatol.*, 2022, **19**, 625–637.

30 M. Bhatia and S. Moochhala, Role of inflammatory mediators in the pathophysiology of acute respiratory distress syndrome, *J. Pathol.*, 2004, **202**, 145–156.

31 J. Bhattacharya and M. A. Matthay, Regulation and repair of the alveolar-capillary barrier in acute lung injury, *Annu. Rev. Physiol.*, 2013, **75**, 593–615.

32 M. A. Matthay, L. B. Ware and G. A. Zimmerman, The acute respiratory distress syndrome, *J. Clin. Invest.*, 2012, **122**, 2731–2740.

33 A. I. Salazar-Puerta, M. A. Rincon-Benavides, T. Z. Cuellar-Gaviria, J. Aldana, G. Vasquez Martinez, L. Ortega-Pineda, D. Das, D. Dodd, C. A. Spencer, B. Deng, D. W. McComb, J. A. Englert, S. Ghadiali, D. Zepeda-Orozco, L. E. Wold, D. Gallego-Perez and N. Higuita-Castro, Engineered Extracellular Vesicles Derived from Dermal Fibroblasts Attenuate Inflammation in a Murine Model of Acute Lung Injury, *Adv. Mater.*, 2023, e2210579, DOI: **10.1002/adma.202210579**.

34 T. Tian, Z. Wang and J. Zhang, Pathomechanisms of Oxidative Stress in Inflammatory Bowel Disease and Potential Antioxidant Therapies, *Oxid. Med. Cell. Longevity*, 2017, **2017**, 4535194.

35 X. O. Yang, A. D. Panopoulos, R. Nurieva, S. H. Chang, D. Wang, S. S. Watowich and C. Dong, STAT3 regulates cytokine-mediated generation of inflammatory helper T cells, *J. Biol. Chem.*, 2007, **282**, 9358–9363.

36 J. Wang, R. Li, Z. Peng, B. Hu, X. Rao and J. Li, HMGB1 participates in LPS-induced acute lung injury by activating the AIM2 inflammasome in macrophages and inducing polarization of M1 macrophages via TLR2, TLR4, and RAGE/NF–κB signaling pathways, *Int. J. Mol. Med.*, 2020, **45**, 61–80.

37 Y. Wang, Y. Wang, J. Ma, Y. Li, L. Cao, T. Zhu, H. Hu and H. Liu, YuPingFengSan ameliorates LPS-induced acute lung injury and gut barrier dysfunction in mice, *J. Ethnopharmacol.*, 2023, **312**, 116452.

38 L. Fei, F. Jifeng, W. Tiantian, H. Yi and P. Linghui, Glycyrrhizin Ameliorate Ischemia Reperfusion Lung Injury through Downregulate TLR2 Signaling Cascade in Alveolar Macrophages, *Front. Pharmacol.*, 2017, **8**, 389.

39 M. P. Fallah, R. L. Chelvarajan, B. A. Garvy and S. Bondada, Role of phosphoinositide 3-kinase-Akt signaling pathway in the age-related cytokine dysregulation in splenic macrophages stimulated via TLR-2 or TLR-4 receptors, *Mech. Ageing Dev.*, 2011, **132**, 274–286.

40 L. Wolf, C. Herr, J. Niederstraßer, C. Beisswenger and R. Bals, Receptor for advanced glycation endproducts (RAGE) maintains pulmonary structure and regulates the response to cigarette smoke, *PLoS One*, 2017, **12**, e0180092.

41 B. J. Grube, C. G. Cochane, R. D. Ye, C. E. Green, M. E. McPhail, R. J. Ulevitch and P. S. Tobias, Lipopolysaccharide binding protein expression in primary human hepatocytes and HepG2 hepatoma cells, *J. Biol. Chem.*, 1994, **269**, 8477–8482.

42 H. Y. Yao, L. H. Zhang, J. Shen, H. J. Shen, Y. L. Jia, X. F. Yan and Q. M. Xie, Cyptoporus polysaccharide prevents lipopolysaccharide-induced acute lung injury associated with down-regulating Toll-like receptor 2 expression, *J. Ethnopharmacol.*, 2011, **137**, 1267–1274.

43 L. Xu, T. Xue, J. Zhang and J. Qu, Knockdown of versican V1 induces a severe inflammatory response in LPS-induced acute lung injury via the TLR2-NF-κB signaling pathway in C57BL/6J mice, *Mol. Med. Rep.*, 2016, **13**, 5005–5012.

44 B. S. Park and J. O. Lee, Recognition of lipopolysaccharide pattern by TLR4 complexes, *Exp. Mol. Med.*, 2013, **45**, e66.

45 M. Vacca, G. Celano, F. M. Calabrese, P. Portincasa, M. Gobbetti and M. De Angelis, The Controversial Role of Human Gut Lachnospiraceae, *Microorganisms*, 2020, **8**, 573.

46 F. Chabot, J. A. Mitchell, J. M. Gutteridge and T. W. Evans, Reactive oxygen species in acute lung injury, *Eur. Respir. J.*, 1998, **11**, 745–757.

47 H. Lv, Q. Liu, Z. Wen, H. Feng, X. Deng and X. Ci, Xanthohumol ameliorates lipopolysaccharide (LPS)-induced acute lung injury via induction of AMPK/GSK3β-Nrf2 signal axis, *Redox Biol.*, 2017, **12**, 311–324.

48 P. Poprac, K. Jomova, M. Simunkova, V. Kollar, C. J. Rhodes and M. Valko, Targeting Free Radicals in Oxidative Stress-Related Human Diseases, *Trends Pharmacol. Sci.*, 2017, **38**, 592–607.

49 S. Bae, X. C. Pan, S. Y. Kim, K. Park, Y. H. Kim, H. Kim and Y. C. Hong, Exposures to particulate matter and polycyclic aromatic hydrocarbons and oxidative stress in schoolchildren, *Environ. Health Perspect.*, 2010, **118**, 579–583.

50 S. Lu, S. Xu, L. Chen, Y. Deng and J. Feng, Periplaneta americana Extract Pretreatment Alleviates Oxidative Stress and Inflammation and Increases the Abundance of Gut Akkermansia muciniphila in Diquat-Induced Mice, *Antioxidants*, 2022, **11**, 1806.

51 S. Xiong, H. Sun, C. Lu, J. He, Z. Wu, Y. Wang and Q. Zheng, Kuqin ameliorates Lipopolysaccharide-induced acute lung injury by regulating indoleamine 2,3-dioxygenase 1 and Akkermansia muciniphila, *Biomed. Pharmacother.*, 2023, **158**, 114073.

52 Z. Wang, J. Liu, F. Li, Y. Luo, P. Ge, Y. Zhang, H. Wen, Q. Yang, S. Ma and H. Chen, The gut-lung axis in severe acute Pancreatitis-associated lung injury: The protection by the gut microbiota through short-chain fatty acids, *Pharmacol. Res.*, 2022, **182**, 106321.

53 B. Han, K. Chao, D. Wang, Y. Sun, X. Ding, X. Zhang, S. Liu, J. Du, Y. Luo, H. Wang, X. Duan, H. Zhao and T. Sun, A purified membrane protein from Akkermansia muciniphila blunted the sepsis-induced acute lung injury by modulation of gut microbiota in rats, *Int. Immunopharmacol.*, 2023, **121**, 110432.

54 S. Kitamoto, H. Nagao-Kitamoto, Y. Jiao, M. G. Gillilland 3rd, A. Hayashi, J. Imai, K. Sugihara, M. Miyoshi, J. C. Brazil, P. Kuffa, B. D. Hill, S. M. Rizvi, F. Wen, S. Bishu, N. Inohara, K. A. Eaton, A. Nusrat, Y. L. Lei, W. V. Giannobile and N. Kamada, The Intermucosal Connection between the Mouth and Gut in Commensal Pathobiont-Driven Colitis, *Cell*, 2020, **182**, 447–462.

55 W. H. Bao, W. L. Yang, C. Y. Su, X. H. Lu, L. He and A. H. Zhang, Relationship between gut microbiota and vascular calcification in hemodialysis patients, *Renal Failure*, 2023, **45**, 2148538.

56 R. Li, R. Liu, L. Chen, G. Wang, L. Qin, Z. Yu and Z. Wan, Microbiota from Exercise Mice Counteracts High-Fat High-Cholesterol Diet-Induced Cognitive Impairment in C57BL/6 Mice, *Oxid. Med. Cell. Longevity*, 2023, **2023**, 2766250.

57 Z. Bao, W. Wang, X. Wang, M. Qian and Y. Jin, Sub-Chronic Difenoconazole Exposure Induced Gut Microbiota Dysbiosis in Mice, *Toxics*, 2022, **10**, 34.

58 J. S. Mar, N. Ota, N. D. Pokorzynski, Y. Peng, A. Jaochico, D. Sangaraju, E. Skippington, A. N. Lekkerkerker, M. E. Rothenberg, M. W. Tan, T. Yi and M. E. Keir, IL-22 alters gut microbiota composition and function to increase aryl hydrocarbon receptor activity in mice and humans, *Microbiome*, 2023, **11**, 47.

59 A. Mohammed, H. K. Alghetaa, J. Zhou, S. Chatterjee, P. Nagarkatti and M. Nagarkatti, Protective effects of Δ(9)-tetrahydrocannabinol against enterotoxin-induced acute respiratory distress syndrome are mediated by modulation of microbiota, *Br. J. Pharmacol.*, 2020, **177**, 5078–5095.

60 Y. F. Ni, J. Wang, X. L. Yan, F. Tian, J. B. Zhao, Y. J. Wang and T. Jiang, Histone deacetylase inhibitor, butyrate, attenuates lipopolysaccharide-induced acute lung injury in mice, *Respir. Res.*, 2010, **11**, 33.

61 A. El Kaoutari, F. Armougom, J. I. Gordon, D. Raoult and B. Henrissat, The abundance and variety of carbohydrate-active enzymes in the human gut microbiota, *Nat. Rev. Microbiol.*, 2013, **11**, 497–504.

62 M. Guerrero Sanchez, S. Passot, S. Campoy, M. Olivares and F. Fonseca, Ligilactobacillus salivarius functionalities, applications, and manufacturing challenges, *Appl. Microbiol. Biotechnol.*, 2022, **106**, 57–80.

63 N. R. Shin, T. W. Whon and J. W. Bae, Proteobacteria: microbial signature of dysbiosis in gut microbiota, *Trends Biotechnol.*, 2015, **33**, 496–503.

64 S. A. Whiteside, J. E. McGinniss and R. G. Collman, The lung microbiome: progress and promise, *J. Clin. Invest.*, 2021, **131**.

65 R. Bingula, M. Filaire, N. Radosevic-Robin, M. Bey, J. Y. Berthon, A. Bernalier-Donadille, M. P. Vasson and E. Filaire, Desired Turbulence? Gut-Lung Axis, Immunity, and Lung Cancer, *J. Oncol.*, 2017, **2017**, 5035371.

66 B. S. Scales, R. P. Dickson and G. B. Huffnagle, A tale of two sites: how inflammation can reshape the microbiomes of the gut and lungs, *J. Leukocyte Biol.*, 2016, **100**, 943–950.

67 S. E. Winter and A. J. Bäumler, Dysbiosis in the inflamed intestine: chance favors the prepared microbe, *Gut Microbes*, 2014, **5**, 71–73.

68 W. Fu, C. Chen, Q. Xie, S. Gu, S. Tao and W. Xue, Pediococcus acidilactici Strain Alleviates Gluten-Induced Food Allergy and Regulates Gut Microbiota in Mice, *Front. Cell. Infect. Microbiol.*, 2022, **12**, 845142.